

## IMMUNOLOGICAL INSIGHTS INTO THE THERAPEUTIC ROLES OF CD24Fc AGAINST SEVERE COVID-19

No-Joon Song, Ph.D.<sup>3</sup>, Carter Allen<sup>1,3,4</sup>, Anna E. Vilgelm, M.D., Ph.D.<sup>3,6,10</sup>, Brian P. Riesenber, Ph.D.<sup>3</sup>, Kevin P. Weller<sup>3</sup>, Kelsi Reynolds<sup>3</sup>, Karthik B. Chakravarthy, B.S.<sup>3,11</sup>, Amrendra Kumar, Ph.D.<sup>6,10</sup>, Aastha Khatiwada, M.S.<sup>5</sup>, Zequn Sun, M.S.<sup>5</sup>, Anjun Ma, Ph.D.<sup>4</sup>, Yuzhou Chang<sup>1,3,4</sup>, Mohamed Yusuf<sup>6</sup>, Anqi Li<sup>1,3,11</sup>, Cong Zeng, Ph.D.<sup>12</sup>, John P. Evans<sup>12</sup>, Donna Bucci<sup>3</sup>, Manuja Gunasena, Ph.D.<sup>8,9</sup>, Menglin Xu, Ph.D.<sup>2</sup>, Namal P.M. Liyanage, Ph.D.<sup>8,9</sup>, Chelsea Bolyard, Ph.D.<sup>3</sup>, Maria Velegriaki, M.D., Ph.D.<sup>3</sup>, Shan-Lu Liu, M.D., Ph.D.<sup>12</sup>, Qin Ma, Ph.D.<sup>4</sup>, Martin Devenport, Ph.D., M.B.A.<sup>13</sup>, Yang Liu, Ph.D.<sup>13</sup>, Pan Zheng, M.D., Ph.D.<sup>13</sup>, Carlos D. Malvestutto, M.D., M.P.H.<sup>2</sup>, Dongjun Chung, Ph.D.<sup>3,4</sup>, and Zihai Li, M.D., Ph.D.<sup>2,3</sup>

### Affiliations:

<sup>1</sup>The Ohio State University, Columbus, OH, USA

<sup>2</sup>Department of Internal Medicine, The Ohio State University College of Medicine, Columbus, OH

<sup>3</sup>The Pelotonia Institute for Immuno-Oncology, The Ohio State University Comprehensive Cancer Center, Columbus, OH, USA

<sup>4</sup>Dept of Biomedical Informatics, The Ohio State University College of Medicine, Columbus, OH

<sup>5</sup>Department of Public Health Sciences, Medical University of South Carolina, Charleston, SC

<sup>6</sup>The Ohio State University Comprehensive Cancer Center, Columbus, OH

<sup>7</sup>Department of Microbiology, The Ohio State University College of Arts and Sciences, Columbus, OH, USA

<sup>8</sup>Department of Microbial Infection and Immunity, The Ohio State University College of Medicine, Columbus, OH, USA

<sup>9</sup>Department of Veterinary Biosciences, The Ohio State University College of Veterinary Medicine, Columbus, OH, USA

<sup>10</sup>Department of Pathology, The Ohio State University College of Medicine, Columbus, OH

<sup>11</sup>The Ohio State University College of Medicine, Columbus, OH, USA

<sup>12</sup>Center for Retrovirus Research and Department of Veterinary Biosciences, The Ohio State University, Columbus, OH, USA

<sup>13</sup>OncoC4, Rockville, MD, USA

N-J.S., C.A., A.V. and B.P.R. are co-first authors. C.D.M., D.C. and Z.L. are co-senior authors.

Address reprint requests to Dr. Zihai Li (corresponding author), Pelotonia Institute for Immunology, The Ohio State University James Comprehensive Cancer Center, Columbus, Ohio 43210, USA, or [zihai.li@osumc.edu](mailto:zihai.li@osumc.edu).

## ABSTRACT

**BACKGROUND.** SARS-CoV-2 causes COVID-19 through direct lysis of infected lung epithelial cells, which releases damage-associated molecular patterns (DAMPs) and induces a pro-inflammatory cytokine milieu causing systemic inflammation. Anti-viral and anti-inflammatory agents have shown limited therapeutic efficacy. Soluble CD24 (CD24Fc) can dampen the broad inflammatory response induced by DAMPs, and a recent randomized phase III trial evaluating impact of CD24Fc in patients with severe COVID-19 has shown encouraging clinical efficacy.

**METHODS.** We studied peripheral blood samples obtained from 22 patients enrolled in the SAC-COVID trial (NCT04317040), which were collected before and at multiple time points after treatment with CD24Fc or placebo. We performed high dimensional spectral flow cytometry analysis and measured cytokine levels to discern the immunological impact of CD24Fc treatment on patients with COVID-19.

**RESULTS.** Patient characteristics from the CD24Fc vs. placebo groups were clinically matched allowing us to compare results without apparent confounding factors. Using high-content spectral flow cytometry, we found systemic hyper-activation of multiple cellular compartments in the placebo group, including CD8<sup>+</sup> T cells, CD4<sup>+</sup> T cells, and CD56<sup>+</sup> NK cells in patients with untreated COVID-19. By contrast, CD24Fc-treated patient samples demonstrated blunted systemic inflammation, with a return to homeostasis in both NK and T cells within days. A single dose of CD24Fc significantly attenuated systemic IL-10 and IL-15 cytokines, and diminished the coexpression and networking among inflammatory cytokines associated with COVID-19.

**CONCLUSIONS.** Our clinical and immunological data supports further development of CD24Fc as a novel therapeutic against severe COVID-19.

## INTRODUCTION

The pathogenesis of SARS-CoV-2 is a multistep process starting with the infection of ACE2-expressing lung epithelial cells<sup>1</sup>. Following infection, unconstrained viral replication leads to cell lysis and the release of DAMPs. Recognition of these molecules by neighboring cells produces a pro-inflammatory milieu through the release of cytokines (such as IL-6 and IL-10), which recruit and activate monocytes, macrophages, and T cells<sup>2</sup>. In severe COVID-19, this pro-inflammatory feedback loop results in a persistent and harmful response that leads to structural damage of the lung. The resulting cytokine storm can lead to acute respiratory distress syndrome (ARDS) and multi-organ failure<sup>3</sup>. While DAMPs can drive systemic inflammation in various settings, whether it occurs in COVID-19 remains unknown.

Interim results from the Solidarity trial (NCT04315948) indicate that several repurposed interventions do not significantly alter COVID-19 morbidity and mortality<sup>4</sup>. Other approaches, including cytokines and convalescent plasma, have also been largely ineffective<sup>5,6</sup>. The anti-inflammatory glucocorticoid dexamethasone is the only intervention shown to reduce mortality in patients with critical-to-severe COVID-19<sup>7</sup>. Thus, effective therapies are needed for these patients.

CD24Fc treatment attenuates inflammation associated with viral infections, autoimmunity, and graft-versus-host diseases<sup>8-10</sup>. In this study, we compared blood samples from COVID-19 patients enrolled in the SAC-COVID trial following CD24Fc or placebo. We examined dynamic changes of peripheral blood mononuclear cells (PBMCs) and systemic cytokine and chemokine levels. We demonstrated that CD24Fc reversed the inflammatory hallmarks associated with severe COVID-19, including cytokine storm and immune activation.

## METHODS

**PATIENTS AND TRIAL PROCEDURE.** This study included samples from patients enrolled in

NCT04317040 at The Ohio State University Wexner Medical Center (patient details described in **Table S1**). Patients eligible for this trial were hospitalized with COVID-19, requiring supplemental oxygen but not mechanical ventilation, with a prior positive SARS-CoV-2 PCR test. Consented and enrolled patients were randomized in a double-blinded fashion to receive either CD24Fc antibody (480 mg IV infusion) or placebo control (IV saline). Peripheral blood samples were collected from patients before (day 1, D1) and after (D2, D4, D8, D15, and D29) treatment. The Western Institutional Review Board approved trial and protocol. The study was monitored by a contract research organization; safety reports were submitted to an independent Data and Safety Monitoring Board. This trial was conducted in compliance with the protocol, International Conference on Harmonization Good Clinical Practice, and all applicable regulatory requirements.

**LABORATORY ASSAYS.** Immune profiling and cytokine/chemokine assays were performed at The Ohio State University, and per manufacturer's instructions as applicable<sup>11,12</sup>. We developed multiple high dimensional spectral flow cytometry panels to study the dynamic changes of CD8<sup>+</sup>, CD4<sup>+</sup>, and CD56<sup>+</sup> immune cell subsets (**Table S2**). See Supplementary Appendix for details.

**BIOINFORMATICS AND STATISTICAL ANALYSIS.** Bioinformatic analyses were performed as previously described<sup>13-21</sup>. Flow cytometry data were preprocessed using the OMIQ software, visualized using the Uniform Manifold Approximation and Projection (UMAP) algorithm, and analyzed using a multivariate t-mixture model<sup>13</sup>. Immune cell activation score was constructed by aggregating pre-selected activation markers<sup>14,15</sup> using a principal component analysis (PCA) applied to the flow cytometry data of HD and baseline COVID-19 patients. Cytokine score was constructed using a weighted sum approach and validated using PCA and autoencoder approaches<sup>16</sup>. Network-level analysis of cytokine data was implemented by constructing a correlation network between cytokines and evaluating the network structure and importance of each node in the network based on an eigenvector centrality (EC) score<sup>20</sup>. Group comparisons

were evaluated using independent sample t-test or Kruskal-Wallis test for continuous variables, and Chi-squared test for categorical variables. Longitudinal analyses were implemented using generalized linear mixed models (GLMMs).

## RESULTS

**POPULATION DYNAMICS OF IMMUNE CELLS.** We utilized a high dimensional spectral flow cytometry panel with an extensive array of immune population markers (**Table S2**) to analyze the systemic effects of SARS-CoV-2 and CD24Fc treatment on PBMCs. Using an unbiased clustering approach based on a multivariate *t*-mixture model<sup>13</sup>, we identified 12 distinct clusters that we visualized in two dimensions using the UMAP algorithm (**Fig 1A**). Using clustered heatmap analysis, we correlated expression intensity with clusters to annotate B cells (clusters 1, 6, 8), CD8<sup>+</sup> T cells (clusters 7, 11, 12), CD4<sup>+</sup> T cells (clusters 2, 3),  $\gamma\delta$  T cells (cluster 4), NK cells (cluster 10), and myeloid cells (clusters 5, 9) (**Fig 1B**). Comparing systemic immune population dynamics (**Fig 1C-D**), we found significant increases in plasma B cells (cluster 6), NK cells (cluster 10), and terminally differentiated CD8<sup>+</sup> T cells (cluster 12) in baseline (D1) COVID-19 patients vs. healthy donors (HD). Conversely, we found that HD samples were enriched for naïve CD8<sup>+</sup> T cells (cluster 11) and a subset of myeloid cells (cluster 5). These initial findings were consistent with established immunopathology of SARS-CoV-2 infection and the important role the adaptive immune system plays in viral pathogen response<sup>22-25</sup>, and thus validated our experimental approach.

We next used UMAP contour plots to investigate the effects of CD24Fc treatment on immune population dynamics over time (**Fig 1E-F**). From baseline to D8, the CD24Fc group displayed a sharp and steady decline of plasma B cells (cluster 6), which coordinated with a proportional increase in mature B cells (cluster 8). The placebo group showed relatively stable cell proportions for these populations over the same time frame.

**CD24Fc SUPPRESSES T CELL ACTIVATION.** We developed a 25-marker flow cytometry panel to examine the intricacies associated with effector cell (NK and CD4<sup>+</sup>/CD8<sup>+</sup> T cell) activation and differentiation in response to SARS-CoV-2 infection and CD24Fc treatment (**Table S2**). Using our unbiased clustering approach, we identified eight distinct clusters within CD8<sup>+</sup> T cells from COVID-19 and HD samples (**Fig 2A-C**). At baseline, COVID-19 samples showed enriched frequency of clusters 4, 5, 7, and 8, which express markers of activation; HD samples were skewed towards cluster 1, which exhibits naive phenotype (**Fig. 2D-E**). To analyze the impact of CD24Fc on CD8<sup>+</sup> T cell activation, we generated UMAP contour plots for each treatment group (**Fig 2F**), and analyzed changes to cluster proportions over time (**Fig 2G**). CD24Fc treatment correlated with a modest increase in cluster 1 frequency over time, whereas placebo-treated patients showed marked decline. Conversely, the proportion of cluster 8 cells (a population whose expression pattern is suggestive of highly activated CD8<sup>+</sup> T cells) were stagnant in CD24Fc-treated patients, compared to the marked increase seen in placebo group (**Fig 2G**).

While tracking cluster proportions over time provides an unbiased global view of the data, these statistically-distinct cell clusters may not always correspond perfectly to biologically-distinct cell types. Therefore, we augmented the unbiased clustering analysis with a semi-supervised approach to define an unbiased CD8<sup>+</sup> T cell activation score. Known markers of T cell activation (T-bet, Ki-67, CD69, TOX, and GZMB) were significantly increased in baseline COVID-19 patients compared to HD (**Fig 2H**), supporting our hypothesis that SARS-CoV-2 infection increases peripheral T cell activation. To create a unified cell-level activation score, we used PCA to implement dimension reduction of the cell-by-activation marker expression data for all baseline COVID-19 and HD cells. The first principal component (PC1) loadings of each activation marker were used as coefficients in a linear model for defining the activation score (**Table S3**). Thus, while we manually selected key T cell activation markers, we determined the relative contribution

of each activation marker to the final activation score in an unbiased and data-adaptive manner, yielding a semi-supervised approach. We observed positive PC1 loadings and positive average log-fold changes for each activation marker, confirming that higher activation scores reflect higher T cell activation (**Table S3**). Distributions of activation scores across cell clusters also confirmed that more highly activated cell subsets feature higher activation scores (**Fig 2I**).

To characterize the effect of CD24Fc treatment on global CD8<sup>+</sup> T cell activation, we adopted a GLMM of the activation scores over time. While CD8<sup>+</sup> T cell activation scores at baseline were not statistically different between groups, the predicted mean activation scores indicate significantly different trajectories between placebo and CD24Fc groups over time (**Fig 2J**). Thus, we conclude that CD24Fc treatment significantly reduced CD8<sup>+</sup> T cell activation compared to placebo. CD4<sup>+</sup> T cell activation also plays an important role in immune response to SARS-CoV-2 infection, so we applied the analysis strategy presented above to this population<sup>22</sup>. To comprehensively understand the role of CD4<sup>+</sup> T cells and FOXP3<sup>+</sup> Tregs, we analyzed total CD4<sup>+</sup> T cells including FOXP3<sup>+</sup> subset (**Fig S1**), and then FOXP3<sup>+</sup> Tregs exclusively (**Fig S2**). Both analyses showed hyperactivated subsets and overall activation score decreased by CD24Fc treatment.

**CD24Fc REDUCES NK CELL ACTIVATION.** The increased number of NK cells in samples from patients with COVID-19 (**Fig 1C-D**, cluster 10) implies they play an important role in SARS-CoV-2 infection. We investigated the activation status of NK cells using our unbiased clustering and visualization approach, and identified 12 statistically-distinct NK cell clusters, which we visualized on heatmaps and UMAPs (**Fig 3A-C**). Cluster 5, the most highly represented cluster in HD samples, displayed an expression pattern suggestive of a less activated population. Samples from COVID-19 patients revealed significant reduction in cluster 5 and expansion of clusters 4, 6, 8, 9, 10, 11, and 12 (**Fig 3D-E**).



To understand the role of CD24Fc treatment on NK cell population dynamics, we generated UMAP contour plots to visualize temporal and treatment-based changes (**Fig 3F**), and quantified these differences (**Fig 3G**). Clusters 1 and 2, which show mild activation, were increased by CD24Fc, while cluster 11, which expresses multiple activation markers, was decreased. To visualize activation, known NK cell activation markers (TOX, GZMB, KLRG1, Ki-67, and LAG3) were assessed (**Fig 3H**) and plotted per cluster (**Fig 3I**). Using a GLMM of activation scores over time, we found that while baseline values for NK cell activation were not statistically different, the mean activation scores were significantly different between placebo and CD24Fc groups throughout the study duration (**Fig 3J**). Thus, CD24Fc treatment rapidly reduced NK cell activation status, and the impact was sustained throughout the study period.

**CD24Fc ATTENUATES SYSTEMIC CYTOKINE RESPONSE.** To examine the effect of CD24Fc on cytokine response to SARS-CoV-2 infection, we compared plasma cytokine concentrations from HD and COVID-19 patients treated with CD24Fc or placebo. We used multiplex ELISA and Luminex analysis platforms testing 37 cytokines in total. Fifteen out of 37 tested cytokines were significantly elevated during SARS-CoV-2 infection (**Fig 4A, Fig S3A**). These included cytokines associated with type 1 (IL-12p40, CXCL9, IL-15) and type 3 (IL-1 $\alpha$ , IL-1 $\beta$ , RANTES) immunity, and chemokine MCP-1 (CCL2) that recruits monocytes and T cells to the sites of inflammation. Only three out of 37 cytokines were significantly downregulated in COVID-19 patients (**Fig S3A**).

We next studied the impact of CD24Fc on cytokine expression in patients with COVID-19. As shown in **Fig 4B**, substantial reduction of cytokines (GM-CSF, IL-5, IL-7, IL-10) and chemokines (MIG, MIP-1 $\alpha$ , MIP-1 $\beta$ ) was observed within 24 hours of CD24Fc. At 1 week after treatment, most of the cytokines and chemokines tested are reduced by 10-fold or more. The majority of them are selectively reduced in the CD24Fc-treated patients including cytokines critically involved in COVID-19 pathogenesis, such as IL-6 and GM-CSF. Analysis of cytokine scores calculated by

integrating expression of all markers tested by multiplex ELISA platform using weighted sum approach demonstrated significant decrease in CD24Fc-treated groups compare to placebo (**Fig 4C**). This finding was independently confirmed using Autoencoder<sup>16</sup> and PCA (**Fig S3D**).

To better understand this modulation, we studied correlations between individual cytokines across groups. Correlation matrices (**Fig 4F**) showed that only a few groups of cytokines were co-expressed by HD. The numbers of co-regulated cytokines dramatically increased in baseline COVID-19 samples indicating activation of coordinated cytokine response. Remarkably, samples from CD24Fc-treated patients (pooled over time) showed a decline in cytokine correlations compared to baseline or placebo treatment. Similarly, cytokine network plots connecting cytokines with moderate and strong associations (Pearson correlation  $r > 0.4$ <sup>17</sup>) showed lower overall interconnectedness in CD24Fc group as compared to baseline or placebo treatment (**Fig 4G**). The overall cytokine network correlations and connectivity in CD24Fc-treated patients were significantly different from baseline or placebo treatment (**Fig 4H-I**).

To understand the relevance of decreased correlation and connectivity of the cytokine network in CD24Fc-treated patients to disease severity and therapeutic effect, we performed a similar analysis using a previously published dataset of cytokine expression in serum from patients with COVID-19 who were either treated in the intensive care unit (ICU patients) or did not require ICU treatment (non-ICU patients)<sup>26</sup>. Notably, we found that inter-cytokine correlation and connectivity was lower in non-ICU patients than ICU patients (**Fig S4**). These data suggest that increased blood cytokine network correlation and connectivity are associated with increased COVID-19 disease severity and ICU treatment, while mild disease (without the need for ICU treatment) is characterized by lower correlation and connectivity. Therefore, decreased correlation and connectivity of the cytokine network in CD24Fc-treated patients are likely evidence of therapeutic efficacy.

To identify factors that may play an important role in response to CD24Fc, we calculated centrality scores<sup>20</sup> for individual cytokines based on their connectivity and correlations within the global cytokine network (**Table S4**). The variances of the centrality scores of 30 cytokines were lower in baseline and placebo-treated COVID-19 patients compared to HD and CD24Fc-treated COVID-19 patients (**Fig 4J**). These data indicate that distinct cytokines are highly heterogeneous in terms of their interconnectedness with other cytokines (centrality) in healthy individuals. Upon SARS-CoV-2 infection, cytokine centralities become more uniform and subsequent CD24Fc treatment abrogates this effect (**Fig 4J**). Centrality scores for individual markers are shown in **Table S4**.

## DISCUSSION

The severe COVID-19 patients studied herein demonstrated accelerated clinical recovery following CD24Fc treatment compared to placebo. CD24Fc was generally well-tolerated, reduced disease progression, and shortened hospital length of stay (results under review in Welker J *et al.* “Therapeutic Efficacy and Safety of CD24Fc in Hospitalised Patients with COVID-19,” submitted to *Lancet*). Given the proposed mechanism of action and pathophysiology of SARS-CoV-2, we hypothesized that CD24Fc reduced the hyperactive systemic immune responses in infected patients leading to accelerated return to homeostasis. Using deep immune profiling of longitudinal samples combined with sophisticated bioinformatic analysis, we uncovered the effects of CD24Fc on the systemic host immune response. Overall, we found that CD24Fc treatment blunted immune cell activation across several compartments and facilitated return to a more normal phenotype following SARS-CoV-2 infection.

Comparing baseline COVID-19 patients with HD allowed us to identify the immune cell populations driving pathogenesis. As expected, we saw a significant increase in activated CD8<sup>+</sup> T and NK cells in SARS-CoV-2-infected patients. We augmented the unbiased clustering analysis

with a semi-supervised approach to define an unbiased activation score. CD24Fc-treated patients demonstrated significant reduction in activation score over time for both CD8<sup>+</sup> T and NK cells compared to placebo-treated patients.

The changes in population dynamics between HD and COVID-19 patients are intriguing and offer two separate interpretations. CD24Fc may preferentially block the differentiation of mature B cells into effector plasma cells, resulting in relatively fewer plasma B cells (cluster 6) and more mature B cells (cluster 8). Alternatively, CD24Fc treatment may reduce the systemic burden of SARS-CoV-2 infection, which would limit the number of plasma cells due to accelerated recovery. As previously shown, higher neutralizing antibodies can reflect severity of disease<sup>27</sup>. In either scenario, the correlation between decreased circulating plasma cells in CD24Fc-treated patient samples suggests significant immuno-modulatory roles in this treatment.

Aberrant and rapid increase in a broad-spectrum of pro-inflammatory cytokines, known as a cytokine storm, plays a central role in pathogenesis of ARDS and other severe complications of SARS-CoV-2 infection<sup>28</sup>. Unlike the cytokine storm associated with immunotherapy, which can be effectively treated by antibodies targeting IL-6R, treating COVID-19 with the same antibodies has shown limited success. Our longitudinal analysis revealed a broad-spectrum up-regulation of systemic cytokines in patients with severe COVID-19. More importantly, CD24Fc treatment cause rapid and sustained reduction of most of the 30 cytokines/chemokines tested. Among them are known COVID-19 therapeutic targets such as IL-6 and GM-CSF. This broad effect may explain the significant therapeutic efficacy of CD24Fc in treating hospitalized COVID-19 patients.

In addition to the two therapeutic targets, we also identified two cytokines that were significantly downregulated after CD24Fc treatment: IL-10 and IL-15. Both are linked with COVID-19 severity, increased intensive care admission, and/or COVID-19-associated death<sup>29-31</sup>. Although generally

associated with immunosuppressive functions, IL-10 can also stimulate NK and CD8<sup>+</sup> T cells and induce B cell proliferation and antibody production<sup>32</sup>. IL-15 promotes activation and expansion of NK and CD8<sup>+</sup> T cells<sup>33,34</sup>. Thus, CD24Fc may blunt NK and CD8<sup>+</sup> T cell activation by suppressing IL-10 and IL-15 production. Since IL-15 also promotes activation and recruitment of neutrophils to site of inflammation, CD24Fc may suppress COVID-19-associated neutrophil activation and/or neutrophilia<sup>35</sup>. Furthermore, CD24Fc may limit viral replication by suppressing IL-10 production, which has been shown to enhance viral replication of HIV, HCV and HBV<sup>36</sup>.

Furthermore, unlike HD, COVID-19 patients displayed strong positive correlations between inflammatory cytokines, consistent with broad misfiring of host immune responses<sup>25,26,37</sup>. Notably, CD24Fc treatment reduced systemic cytokine levels and diminished correlations and connectivity in SARS-CoV-2-infected individuals, thus reshaping the systemic cytokine network towards a less tightly co-regulated state characteristic of homeostasis. Based on analysis of the global cytokine landscape, we conclude that CD24Fc mitigates the exacerbated host systemic inflammatory responses to SARS-CoV-2. This conclusion was corroborated by the decrease of cytokine correlation and connectivity in patients with mild COVID-19 infections as compared to patients with severe disease that required an ICU treatment. A detailed investigation of individual inflammatory markers revealed potential mechanisms of COVID-19 severity reduction by CD24Fc.

In conclusion, the data presented here offer unique immunological insights that underscore the clinical findings of the SAC-COVID trial. These results strongly support further investigation of CD24Fc for various inflammatory conditions including COVID-19. Our unique cytokine centrality analysis and cellular activation index also warrants further study as a prognostic tool for guiding therapy in COVID-19 and other systemic inflammatory conditions.

This work was supported in part by National Institutes of Health (NIH) grants, including R01AI077283, R01CA213290 to Z.L.; and R37CA233770 to A.E.V. Z.L is also supposed by funding from the Pelotonia Foundation. Research reported in this publication was also supported by The Ohio State University Comprehensive Cancer Center and the NIH under grant number P30 CA016058.

We acknowledge the patients who agreed to participate in this clinical trial, as the forward trajectory of science hinges on their support. We acknowledge Oncoimmune (now part of Merck & Co., Inc., Kenilworth, NJ, USA) for designing and supporting the clinical trial, which allowed us to collect samples for our correlative studies. The correlative studies were not part of the original phase III Oncoimmune trial, but were done at The Ohio State University trial site after communication of intent and sample collection. We thank the staff and researchers in the Pelotonia Institute for Immuno-Oncology for their support during the course of the study. We appreciate the expert administrative support by Ms. Teresa Kutcher.

## REFERENCES

1. Hoffmann M, Kleine-Weber H, Schroeder S, et al. SARS-CoV-2 Cell Entry Depends on ACE2 and TMPRSS2 and Is Blocked by a Clinically Proven Protease Inhibitor. *Cell* 2020;181:271-80 e8.
2. Cicco S, Cicco G, Racanelli V, Vacca A. Neutrophil Extracellular Traps (NETs) and Damage-Associated Molecular Patterns (DAMPs): Two Potential Targets for COVID-19 Treatment. *Mediators Inflamm* 2020;2020:7527953.
3. Cao X. COVID-19: immunopathology and its implications for therapy. *Nat Rev Immunol* 2020;20:269-70.
4. Consortium WHOST, Pan H, Peto R, et al. Repurposed Antiviral Drugs for Covid-19 - Interim WHO Solidarity Trial Results. *N Engl J Med* 2021;384:497-511.
5. Simonovich VA, Burgos Pratz LD, Scibona P, et al. A Randomized Trial of Convalescent Plasma in Covid-19 Severe Pneumonia. *N Engl J Med* 2021;384:619-29.
6. Stone JH, Frigault MJ, Serling-Boyd NJ, et al. Efficacy of Tocilizumab in Patients Hospitalized with Covid-19. *N Engl J Med* 2020;383:2333-44.
7. Group RC, Horby P, Lim WS, et al. Dexamethasone in Hospitalized Patients with Covid-19. *N Engl J Med* 2021;384:693-704.
8. Tian RR, Zhang MX, Zhang LT, et al. CD24 and Fc fusion protein protects SIVmac239-infected Chinese rhesus macaque against progression to AIDS. *Antiviral Res* 2018;157:9-17.
9. Liu Y, Zheng P. CD24: a genetic checkpoint in T cell homeostasis and autoimmune diseases. *Trends Immunol* 2007;28:315-20.
10. Toubai T, Hou G, Mathewson N, et al. Siglec-G-CD24 axis controls the severity of graft-versus-host disease in mice. *Blood* 2014;123:3512-23.
11. Park LM, Lannigan J, Jaimes MC. OMIP-069: Forty-Color Full Spectrum Flow Cytometry Panel for Deep Immunophenotyping of Major Cell Subsets in Human Peripheral Blood. *Cytometry A* 2020;97:1044-51.
12. Zeng C, Evans JP, Pearson R, et al. Neutralizing antibody against SARS-CoV-2 spike in COVID-19 patients, health care workers, and convalescent plasma donors. *JCI Insight* 2020;5.
13. Lo K, Brinkman RR, Gottardo R. Automated gating of flow cytometry data via robust model-based clustering. *Cytometry A* 2008;73:321-32.
14. Scott AC, Dundar F, Zumbo P, et al. TOX is a critical regulator of tumour-specific T cell differentiation. *Nature* 2019;571:270-4.
15. Kallies A, Good-Jacobson KL. Transcription Factor T-bet Orchestrates Lineage Development and Function in the Immune System. *Trends Immunol* 2017;38:287-97.
16. Liou C-Y, Cheng W-C, Liou J-W, Liou D-R. Autoencoder for words. *Neurocomputing* 2014;139:84-96.
17. Schober P, Boer C, Schwarte LA. Correlation Coefficients: Appropriate Use and Interpretation. *Anesth Analg* 2018;126:1763-8.

18. Gao J, Tarcea VG, Karnovsky A, et al. Metscape: a Cytoscape plug-in for visualizing and interpreting metabolomic data in the context of human metabolic networks. *Bioinformatics* 2010;26:971-3.
19. Shannon P, Markiel A, Ozier O, et al. Cytoscape: a software environment for integrated models of biomolecular interaction networks. *Genome Res* 2003;13:2498-504.
20. Valente TW, Coronges K, Lakon C, Costenbader E. How Correlated Are Network Centrality Measures? *Connect (Tor)* 2008;28:16-26.
21. Tang Y, Li M, Wang J, Pan Y, Wu FX. CytoNCA: a cytoscape plugin for centrality analysis and evaluation of protein interaction networks. *Biosystems* 2015;127:67-72.
22. Chen Z, John Wherry E. T cell responses in patients with COVID-19. *Nat Rev Immunol* 2020;20:529-36.
23. Laing AG, Lorenc A, Del Molino Del Barrio I, et al. A dynamic COVID-19 immune signature includes associations with poor prognosis. *Nat Med* 2020;26:1623-35.
24. Weiskopf D, Schmitz KS, Raadsen MP, et al. Phenotype and kinetics of SARS-CoV-2-specific T cells in COVID-19 patients with acute respiratory distress syndrome. *Sci Immunol* 2020;5.
25. Mathew D, Giles JR, Baxter AE, et al. Deep immune profiling of COVID-19 patients reveals distinct immunotypes with therapeutic implications. *Science* 2020;369.
26. Lucas C, Wong P, Klein J, et al. Longitudinal analyses reveal immunological misfiring in severe COVID-19. *Nature* 2020;584:463-9.
27. Garcia-Beltran WF, Lam EC, Astudillo MG, et al. COVID-19-neutralizing antibodies predict disease severity and survival. *Cell* 2021;184:476-88 e11.
28. Leisman DE, Ronner L, Pinotti R, et al. Cytokine elevation in severe and critical COVID-19: a rapid systematic review, meta-analysis, and comparison with other inflammatory syndromes. *Lancet Respir Med* 2020;8:1233-44.
29. Angioni R, Sanchez-Rodriguez R, Munari F, et al. Age-severity matched cytokine profiling reveals specific signatures in Covid-19 patients. *Cell Death Dis* 2020;11:957.
30. Abers MS, Delmonte OM, Ricotta EE, et al. An immune-based biomarker signature is associated with mortality in COVID-19 patients. *JCI Insight* 2021;6.
31. Han H, Ma Q, Li C, et al. Profiling serum cytokines in COVID-19 patients reveals IL-6 and IL-10 are disease severity predictors. *Emerg Microbes Infect* 2020;9:1123-30.
32. Wilson EB, Brooks DG. The role of IL-10 in regulating immunity to persistent viral infections. *Curr Top Microbiol Immunol* 2011;350:39-65.
33. Younes SA, Freeman ML, Mudd JC, et al. IL-15 promotes activation and expansion of CD8+ T cells in HIV-1 infection. *J Clin Invest* 2016;126:2745-56.
34. Verbist KC, Klonowski KD. Functions of IL-15 in anti-viral immunity: multiplicity and variety. *Cytokine* 2012;59:467-78.
35. Cassatella MA, McDonald PP. Interleukin-15 and its impact on neutrophil function. *Curr Opin Hematol* 2000;7:174-7.
36. Brooks DG, Trifilo MJ, Edelmann KH, Teyton L, McGavern DB, Oldstone MB. Interleukin-10 determines viral clearance or persistence in vivo. *Nat Med* 2006;12:1301-9.



37. Chevrier S, Zurbuchen Y, Cervia C, et al. A distinct innate immune signature marks progression from mild to severe COVID-19. *Cell Rep Med* 2021;2:100166.

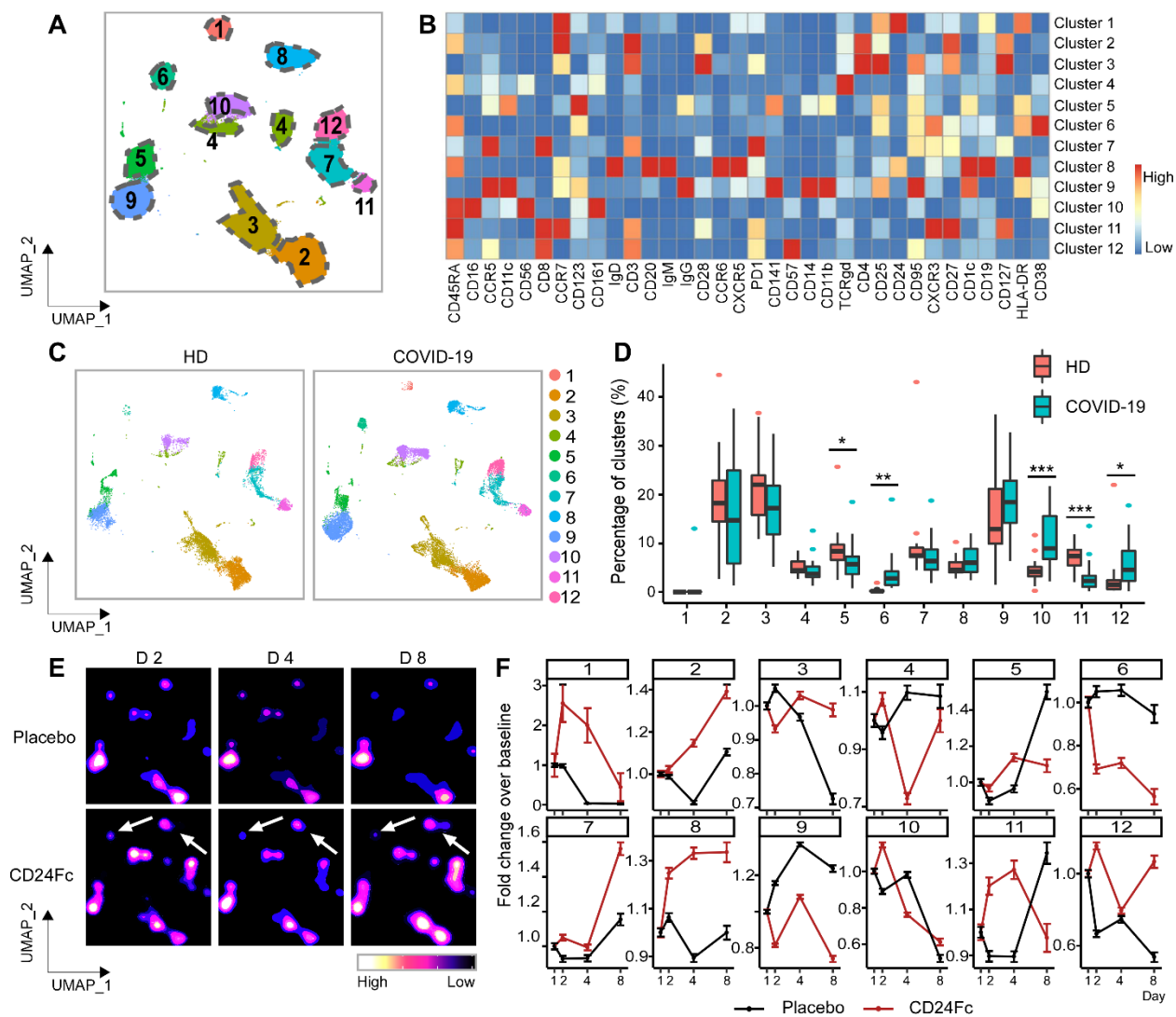


**Figure 1. Population dynamics of peripheral blood mononuclear cells from healthy donors vs. patients with COVID-19 treated with placebo or CD24Fc.** A total of 1,306,473 PBMCs from HD (n=17) and COVID-19 patients (n=22) were clustered using an unbiased multivariate *t*-mixture model, which identified 12 sub-clusters that reflect statistically distinct cell states. Visualization of the relative similarity of each cell and cell cluster on the two-dimensional UMAP space with a 10% downsampling (**Panel A**). Cluster-by-marker heatmap characterizing the expression patterns of individual clusters (**Panel B**). UMAP dot plots (**Panel C**) and cluster frequencies (**Panel D**) of HD vs. baseline COVID-19 patient samples (cluster 5,  $p=0.03$ ; cluster 6,  $p=0.001$ ; cluster 10,  $p<0.001$ ; cluster 11,  $p<0.001$ ). Contour plots representing the density of cells throughout regions of the

UMAP space from COVID-19 patients D2, D4, and D8 after CD24Fc vs. placebo treatment (**Panel E**, white arrows indicate visual changes between CD24Fc vs. placebo contour plots). Selected cluster population dynamics as fold change over baseline for each group over time (**Panel F**) (D2: placebo n=12, CD24Fc n=10; D4: placebo n=11, CD24Fc n=9; D8: placebo n=4, CD24Fc n=3). The p-value was calculated using the Kenward-Roger method. \*, p<0.05; \*\*, p<0.01; \*\*\*, p<0.001.

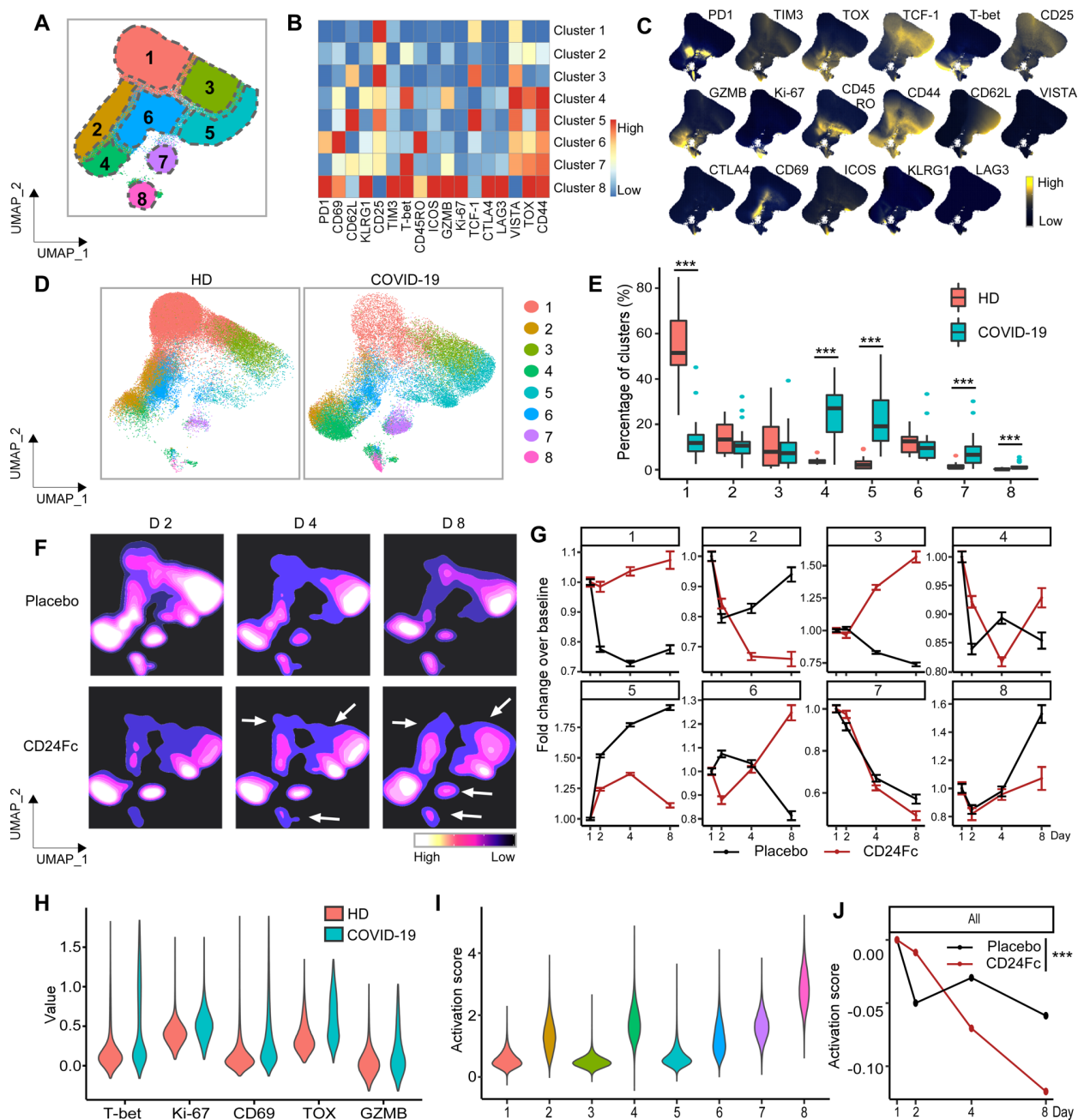


**Figure 2. Subcluster analysis of peripheral blood CD8<sup>+</sup> T cells in COVID-19 patients: activation following SARS-CoV2 infection is dampened by CD24Fc treatment.** A total of 1,466,822 CD8<sup>+</sup> cells from HD (n=17) and COVID-19 (n=22) patients were clustered using an unbiased multivariate *t*-mixture model, which identified 8 CD8<sup>+</sup> sub-clusters that reflect statistically distinct CD8<sup>+</sup> T cell activation states. The relative similarity of each cell and cell cluster on the two-dimensional UMAP space were visualized with a 10% downsampling (**Panel A**). Using

median expression of flow cytometry markers, a cluster-by-marker heatmap was generated to characterize the subsets (**Panel B**) and visualize individual marker expression patterns on the UMAP space (**Panel C**). To understand the effect of SARS-CoV2 infection on cell population dynamics, a comparison was made with UMAP dot plots (**Panel D**) and cluster frequencies (**Panel E**) of HD vs. baseline COVID-19 patient samples (cluster 1,  $p < 0.001$ ; cluster 4,  $p < 0.001$ ; cluster 5,  $p < 0.001$ ; cluster 7,  $p < 0.001$ ; cluster 8,  $p < 0.001$ ). The samples from COVID-19 patients 2, 4, and 8 days after CD24Fc vs. placebo treatment were displayed using contour plots to represent the density of cells throughout regions of the UMAP space (**Panel F**, white arrows indicate visual changes between CD24Fc vs. placebo contour plots). The cluster population dynamics as fold change over baseline in each treatment group was shown (**Panel G**; sample distribution described in **Fig 1F** legend). To better characterize the activation status of CD8 T cells, a subset of markers (T-bet, Ki-67, CD69, TOX, GZMB) was linearly transformed to create a univariate cell-level activation score (**Panel H**), where highly activated cell clusters (such as cluster 8) had highest activation scores (**Panel I**). A GLMM was then fit to the longitudinal cell-level activation scores to assess the effect of CD24Fc treatment on activation scores over time (**Panel J**). The p-value was calculated using the Kenward-Roger method. \*\*\*,  $p < 0.001$ .

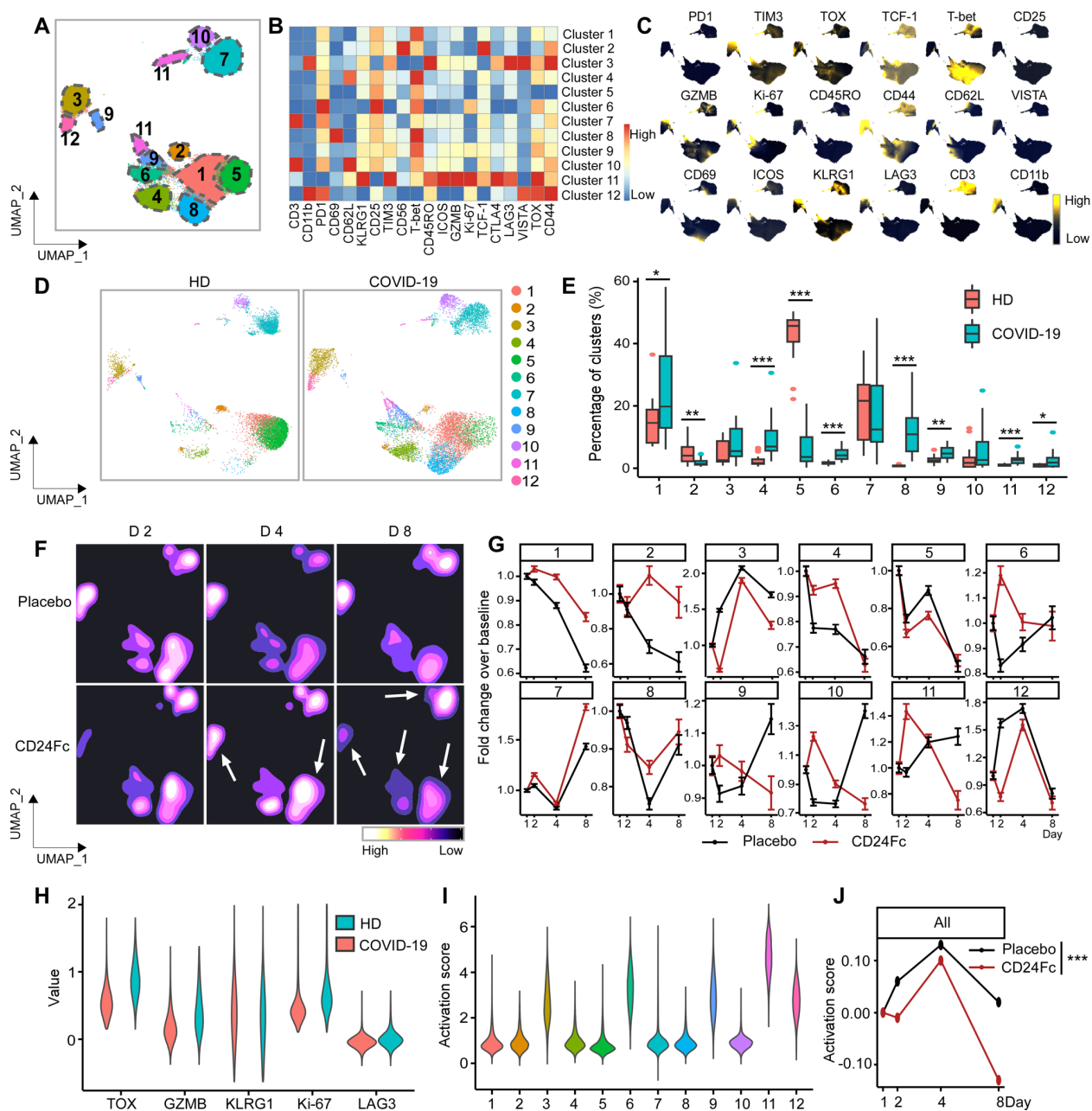


**Figure 3. Subcluster analysis of peripheral blood NK cells in COVID-19 patients: activation of following SARS-CoV2 infection is dampened by CD24Fc treatment.** CD56<sup>+</sup> cells (n=783,623) from HD (n=17) and COVID-19 (n=22) patients were clustered using an unbiased multivariate *t*-mixture model, which identified 12 sub-clusters that reflect statistically distinct CD56<sup>+</sup> T cell activation states. The relative similarity of each cell and cell cluster on the two-dimensional UMAP space were visualized with a 10% downsampling (**Panel A**). Using median

expression of flow cytometry markers, a cluster-by-marker heatmap were generated to characterize the subsets (**Panel B**) and visualize individual marker expression patterns on the UMAP space (**Panel C**). To understand the effect of SARS-CoV2 infection on NK cell population dynamics, a comparison was made with UMAP dot plots (**Panel D**) and cluster frequencies (**Panel E**) of HD vs. baseline COVID-19 patient samples. The day 2, 4, 8 samples from placebo and CD24Fc-treated patient groups were visualized using contour plots to represent the density of cells throughout regions of the UMAP space (**Panel F**, white arrows indicate visual changes between CD24Fc vs. placebo contour plots). The cluster population dynamics as fold change over baseline in each treatment group was shown (**Panel G**; sample distribution described in **Fig 1** legend). To better characterize the activation status of NK cells, a subset of markers (TOX, GZMB, KLRG1, Ki-67, LAG-3) was linearly transformed to create a univariate cell-level activation score (**Panel H**), where highly activated cell clusters (such as cluster 11) had highest activation scores (**Panel I**). A GLMM was then fit to the longitudinal cell-level activation scores to assess the effect of CD24Fc treatment on activation scores over time (**Panel J**). The p-value was calculated using the Kenward-Roger method. \*,  $p < 0.05$ ; \*\*,  $p < 0.01$ ; \*\*\*,  $p < 0.001$ .

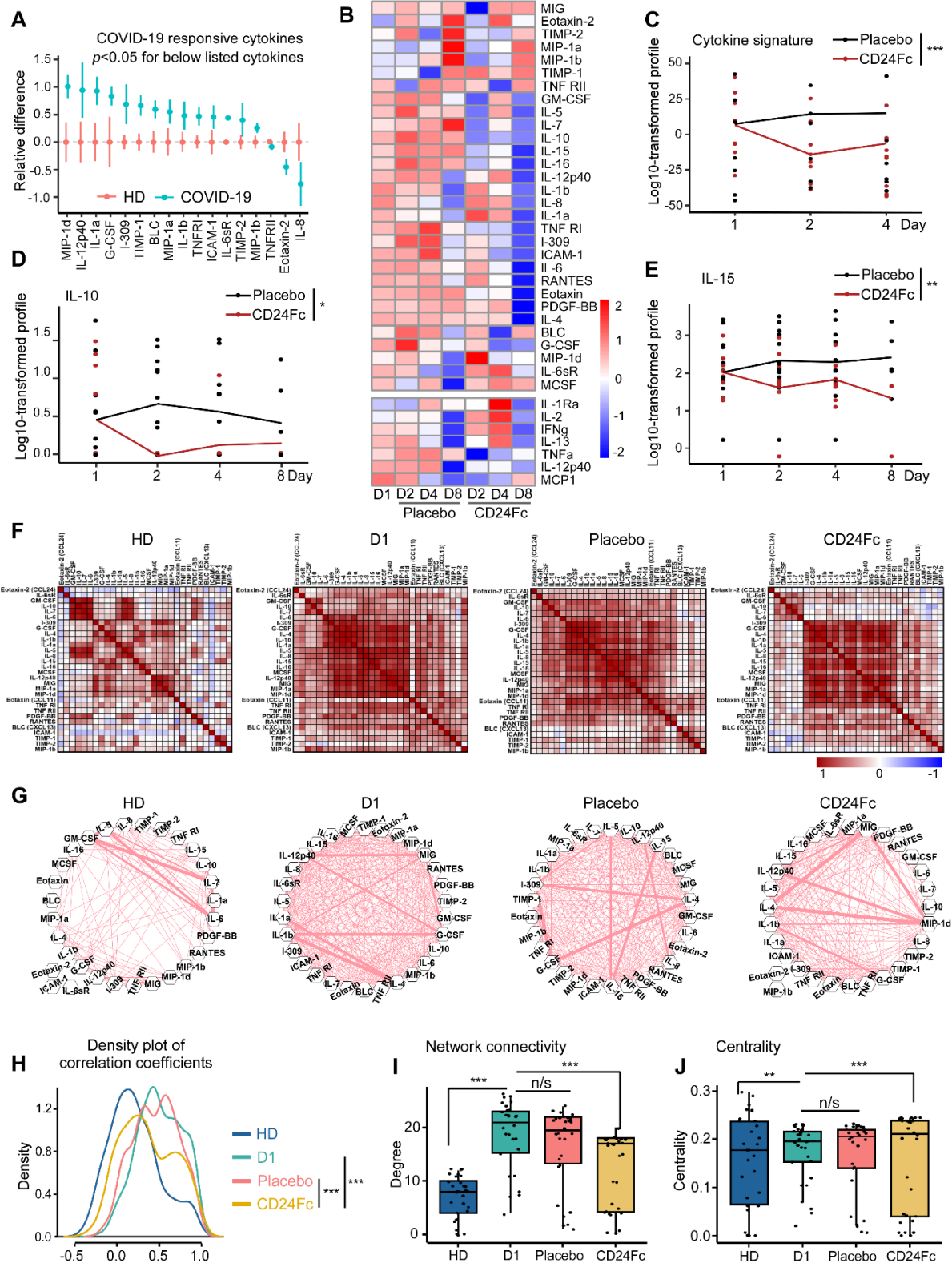




**Figure 4. CD24Fc treatment downregulates systemic cytokine response in patients with COVID-19.** The relative differences in plasma concentrations of cytokines/chemokines between HD (n=25) and COVID-19 patients (n=22) is shown. Values were log-transformed and evaluated using independent sample t-test. Only significantly up- and down-regulated markers are shown (**Panel A**). The heatmap analysis (**Panel B**) was used to visualize the relative levels of plasma cytokines/chemokines in placebo vs. CD24Fc-treated patients at indicated time points (Placebo: D1 n=12, D2 n=12, D4 n=11, D8 n=5; CD24Fc: D1 n=10, D2 n=10, D4 n=9, D8 n=3). To compare longitudinal patterns across groups, each cytokine had its group-specific baseline mean adjusted to match the overall mean at D1 and consequent time points are normalized accordingly, followed by scaling-by-row. The cytokine score was analyzed longitudinally using weighed sum approach (**Panel C**;  $p < 0.001$ ). Using log-10 transformation of cytokine concentrations (dots) and GLMM predicted fixed effects trends (lines), the changes in IL-10 (**Panel D**;  $p = 0.05$ ) and IL-15 (**Panel E**;  $p = 0.002$ ) levels in CD24Fc (red) and placebo (black) groups were revealed. Values and trend lines were centered at D1 mean. The p-value was calculated using the Kenward-Roger method. Using Pearson correlation matrices (**Panel F**; darker red indicates stronger correlation) and network maps (**Panel G**; weight of edge represents correlation coefficient), 30 plasma markers in HD (n=25), COVID-19 baseline (D1, n=22), placebo (pooled D2-D8, n=28), and CD24Fc-treated (pooled D2-D8, n=24) groups were visualized. Using these correlation coefficients, a density plot between 30 plasma cytokines (**Panel H**; D1 vs placebo,  $p = 0.07$ ; D1 vs CD24Fc,  $p < 0.001$ ; placebo vs CD24Fc,  $p < 0.001$ ) was constructed. Kolmogorov-Smirnov test was used to evaluate equality of densities between groups. Analysis of connectivity (**Panel I**) and centrality analysis of cytokine network (**Panel J**) display the cytokine expression relationships within each group. Network connectivity plots display highly correlated connections for each cytokine (i.e., node degree) and evaluated using paired t-test. Centrality analysis of cytokine network used eigenvector centrality score that considers global network connectivity and correlation coefficients between cytokines (HD vs D1,  $p < 0.001$ ; D1 vs placebo,  $p = 0.08$ ; D1 vs CD24Fc,  $p < 0.001$ ). Bartlett's test was

performed to evaluate the significance of variance of centrality scores (HD vs D1,  $p=0.013$ ; D1 vs placebo,  $p=0.17$ ; D1 vs CD24Fc,  $p=0.008$ ). Each dot in Panel I and J represents a cytokine. \*,  $p<0.05$ ; \*\*,  $p<0.01$ ; \*\*\*,  $p<0.001$ .